








# Numerical Simulation of Elasto-Plastic Behavior of Isotropic Composite Materials

Anton Karvatskii , Ihor Mikulionok , Serhii Leleka  ,  
and Vladyslav Solovei 

National Technical University of Ukraine “Igor Sikorsky Kyiv Polytechnic Institute”, 37, Peremohy Ave., Kiev 03056, Ukraine  
sleleka@rst.kpi.ua

**Abstract.** Tools in the form of methodology and software for the numerical study of the thermal-elastoplastic state of coke-pitch composites using the example of isostatic graphite production technology have been developed. A closed mathematical formulation and a method for numerically solving an elastoplastic problem with isotropic hardening based on an implicit inverse mapping algorithm are considered. Using the finite element method, the corresponding program code was developed and verified. A comparison of the results with the data of numerical analysis obtained using the ANSYS Mechanical APDL software product shows that, with isotropic hardening, the maximum discrepancy does not exceed 1.13%, and for ideal plasticity, it is no more than 3.58%. The calculations of the thermal-elastoplastic behavior of the coke-pitch composite in the technological stage of the production of isostatic graphite blanks are performed. It is shown that in the case of non-compliance with the temperature regimes at the initial stages of roasting, plastic deformations occur in the isostatic graphite blanks, which lead to cracking and deterioration of the uniformity of the physical properties of the finished products.

**Keywords:** Composite material · Elastoplasticity · Numerical analysis · Implicit algorithm · Isostatic graphite

## 1 Introduction

One of the composite materials with properties close to isotropic can include coke-pitch mixtures, which are the basis for the production of isostatic graphite (IG) [1, 2]. The composition of these mixtures includes pitch (matrix) and fine (30–150  $\mu\text{m}$ ) or fine-grained (10–30  $\mu\text{m}$ ) filler – coke [3, 4]. Owing to the uniqueness of the physicochemical properties, isostatic graphite has been extremely widely used in various fields of science and technology: from metallurgy and mechanical engineering to atomic and renewable energy [5, 6]. The technological cycle of industrial production of isostatic graphite is divided into the following stages: the first stage is the selection, preparation of raw materials, the preparation of a coke-pitch mixture (composite), as well as the isostatic pressing of “green” blanks, the second stage is the burning of blanks and the third is graphitization [4, 6]. The plastic properties of the composite material for the production of isostatic graphite are shown at the stages of pressing and burning [4, 7].

## 2 Literature Review

Available literature does not contain information on the results of modeling the elastic-plastic behavior of coke-pitch composites at the stages of the production of isostatic graphite blanks, and the mechanical properties are mainly given in the certificates of manufacturers and only for the finished product, which may be associated with the high commercial potential of this technology. In [7, 8], based on well-known analytical solutions for the normal components of the thermal stress tensor in a cylindrical body, the limiting radial temperature differences in composite graphite billets were estimated at the burning stage.

One of the first significant works devoted to implicit algorithms for solving elastoplastic problems is an article by Simo and Taylor [9], which introduced such important concepts as sequential tangential operators and the inverse mapping algorithm. It is shown that for the case independent of the speed of the elastoplastic behavior of the material, the so-called inverse mapping algorithms ensure that the quadratic velocity of the asymptotic convergence of the schemes of iterative solutions based on the Newton method is preserved. In this work, examples of numerical solutions of problems with isotropic and kinematic hardening for the associative flow law are given, as well as a problem with the non-associative Drucker-Prager flow law.

The theoretical foundations for solving a wide class of elastoplastic problems using various modifications of the inverse mapping algorithm are most fully described in [10, 11]. The paper [12] presents a mathematical formulation of the problem of the elastic-plastic state of bulk material based on the classical Drucker-Prager model. Using the inverse mapping algorithm, numerical experiments were carried out using an example of a material characterized by an associative flow law for various values of the angle of repose.

In the considered works [9–12], there are no closed formulations of the problems of thermo-elastic plasticity of composite materials and examples of their numerical implementation that could be directly applied to improve the technology for producing isostatic graphite.

In connection with the foregoing, this work is aimed at developing tools for the numerical study of the elastoplastic state of coke-pitch composites using isostatic graphite technology.

## 3 Research Methodology

### 3.1 Mathematical Statement of the Problem

According to the incremental theory of plasticity, the mathematical model of the isotropic material independent of the speed of the elastoplastic behavior of the isotropic material includes the equilibrium equation, the generalized Hooke law, and the geometric equation written through increments of physical quantities [10–12]:

$$\begin{cases} \nabla \cdot \hat{\boldsymbol{\sigma}} + \rho \hat{\mathbf{b}} = 0; \\ \hat{\boldsymbol{\sigma}} = \frac{E}{1+\nu} \left( \hat{\boldsymbol{\varepsilon}} + \frac{\nu}{1-2\nu} \text{tr}(\hat{\boldsymbol{\varepsilon}}) \hat{\mathbf{I}} \right) - \hat{\boldsymbol{\sigma}}^0; \\ \hat{\boldsymbol{\varepsilon}} = \frac{1}{2} (\nabla \hat{\mathbf{u}} + \hat{\mathbf{u}} \nabla) = \hat{\boldsymbol{\varepsilon}}^{el} + \hat{\boldsymbol{\varepsilon}}^{pl}, \end{cases} \quad (1)$$

where  $\dot{\hat{\boldsymbol{\sigma}}}$  is symmetric stress increment tensor of the second rank, Pa;  $\rho$  is density, kg/m<sup>3</sup>;  $\dot{\mathbf{b}}$  is vector increment of mass forces, N/kg;  $E$  is the modulus of elasticity under uniaxial tension (compression), Pa;  $\nu$  is Poisson's ratio;  $\dot{\hat{\boldsymbol{\epsilon}}}$  is symmetric increment tensor of the total deformations of the second rank;  $\hat{\mathbf{I}}$  is unit tensor of the second rank;  $\text{tr}()$  is tensor trace operator;  $\dot{\hat{\boldsymbol{\sigma}}}^0$  is increment tensor of initial stresses, Pa;  $\dot{\hat{\boldsymbol{\epsilon}}}^{el}$ ,  $\dot{\hat{\boldsymbol{\epsilon}}}^{pl}$  are the elastic and plastic components of the tensor of the increment of total deformations  $\dot{\hat{\boldsymbol{\epsilon}}}$ , respectively;  $\dot{\mathbf{u}}$  is the displacement increment vector, m.

In the case of isotropic hardening, the material yield condition takes the following form [10, 11]

$$F(\hat{\boldsymbol{\sigma}}, \boldsymbol{\varepsilon}_{eq}^{pl}) = \sigma_{eq} - \sigma_y(\sigma_{y0}, \boldsymbol{\varepsilon}_{eq}^{pl}), \tag{2}$$

where  $F$  is the function of the surface fluidity of the material;  $\sigma_{eq}$  is Mises equivalent stress, Pa;  $\sigma_y(\sigma_{y0}, \boldsymbol{\varepsilon}_{eq}^{pl})$  is yield point of the material, taking into account isotropic hardening according to the linear law, Pa;  $\boldsymbol{\varepsilon}_{eq}^{pl}$  is Mises equivalent plastic deformation;  $\sigma_{y0}$  is the initial value of the yield strength of the material, Pa.

The initial conditions for (1) and (2)

$$\dot{\hat{\boldsymbol{\sigma}}}^0 = 0. \tag{3}$$

The boundary conditions for (1) and (2):

- displacement vector

$$\mathbf{u}|_{S_u} = 0, \tag{4}$$

where  $S_u$  is the surface (or surface point) on which the components of displacement are specified, m<sup>2</sup>;

- symmetry

$$\mathbf{n} \cdot \mathbf{u}|_{S_{su}} = 0, \tag{5}$$

where  $\mathbf{n}$  is the vector of the external normal to the surface of the body;  $S_{su}$  is surface symmetry of the body, m<sup>2</sup>;

- external pressure

$$(\hat{\boldsymbol{\sigma}} \cdot \mathbf{n}) \cdot \mathbf{n}|_{S_p} = p, \tag{6}$$

where  $p$  is the external pressure set on the surface of the body  $S_p$ , Pa.

### 3.2 The Methodology of Numerical Research

Consider the theoretical foundations of the implicit Return-Mapping Algorithms [10, 11] using the example of solving the problem of the elastic-plastic behavior of isotropic

material. In the case of the occurrence of elastoplastic deformations in the material, taking into account the temperature load, elastic stresses are determined by the equation

$$\hat{\sigma} = \overset{4}{\hat{C}} : (\hat{\varepsilon}^{tr} - \hat{\varepsilon}^{pl} - \hat{\varepsilon}_T), \quad (7)$$

where  $\overset{4}{\hat{C}}$  is the fourth-rank tensor of the elastic constants of the material, Pa;  $\hat{\varepsilon}^{tr}$  is a tensor of test (full) deformations of the second rank, which is determined in the approximation of an elastic medium;  $\hat{\varepsilon}_T(\beta, T, T_{ref})$  is temperature strain tensor;  $\beta$  is coefficient of linear thermal expansion (CLThE), K<sup>-1</sup>;  $T, T_{ref}$  are the current absolute temperature and the absolute reference temperature, respectively, K.

Under the associative law of plastic flow, the increment of plastic deformations is determined by the relation

$$\Delta \hat{\varepsilon}^{pl} = \Delta \lambda \hat{\mathbf{m}}, \quad (8)$$

where  $\Delta \hat{\varepsilon}^{pl}$  is an increment of plastic deformation at the  $i$ -th step of loading;  $\Delta \lambda$  is the scalar associative factor (plasticity coefficient), which is determined by the formula

$$\Delta \lambda = \frac{\hat{\mathbf{m}} : \overset{4}{\hat{C}} : \hat{\varepsilon}^{tr}}{\hat{\mathbf{m}} : \overset{4}{\hat{C}} : \hat{\mathbf{m}}^{T+h}}, \quad (9)$$

where  $\hat{\mathbf{m}}$  is the derivative of the plasticity function (2) with respect to the stress tensor;  $h$  is hardening module, Pa.

Using the inverse Euler method, Eq. (7), taking into account (8) and (9) for  $k+1$  the loading step, can be easily transformed to

$$\hat{\sigma}^{k+1} = \hat{\sigma}^{tr} - \Delta \lambda^{k+1} \overset{4}{\hat{C}} : \hat{\mathbf{m}}(\hat{\sigma}^{k+1}), \quad (10)$$

where  $\hat{\sigma}^{k+1}$  is the elastic stress tensor at the loading step, Pa;  $\hat{\sigma}^{tr}$  is test stress tensor determined in the approximation of an elastic body, Pa.

Formula (10) describes the mapping of the test stress tensor in the direction of the yield surface  $F$ . Therefore, this method of solving the elastic-plasticity problem is called the inverse mapping algorithm [10].

System of Eqs. (10), taking into account the symmetry of the stress tensor, has seven unknowns, i.e. six independent components  $\hat{\sigma}^{tr}$  and plasticity coefficient  $\Delta \lambda$ . In this regard, to close the system of Eqs. (10), it is necessary to supplement it with a scalar Eq. (2) of the form

$$F(\widehat{\boldsymbol{\sigma}}^{k+1}, \Delta\lambda) = 0. \tag{11}$$

Equation (11) ensures the fulfillment of the yield condition at the end of each  $k$ -th stage of loading.

To apply the Newton method, the nonlinear system of Eqs. (10), (11) must be rewritten in the residual format (12). Moreover, to represent the tensors  $\widehat{\boldsymbol{\sigma}}^{k+1}$ ,  $\widehat{\boldsymbol{\sigma}}^{tr}$  and  $\widehat{\mathbf{m}}$  in the form of vectors, it is necessary to make the transition to six-dimensional space, taking into account their symmetry. This makes it possible to replace tensors of the second rank  $\widehat{\boldsymbol{\sigma}}^{k+1}$ ,  $\widehat{\boldsymbol{\sigma}}^{tr}$  and  $\widehat{\mathbf{m}}$  with the corresponding vectors  $\boldsymbol{\sigma}^{k+1}$ ,  $\boldsymbol{\sigma}^{tr}$  and  $\mathbf{m}$  with six components, and instead of using the tensor of the fourth rank  $\widehat{\mathbf{C}}$  use the tensor of the second rank of elastic constants  $\widehat{\mathbf{D}}^{el}$  of dimension six:

$$\begin{cases} \mathbf{r}_\sigma = \boldsymbol{\sigma}^{k+1} - \boldsymbol{\sigma}^{tr} + \Delta\lambda^{k+1} \widehat{\mathbf{D}}^{el} \cdot \mathbf{m}(\boldsymbol{\sigma}^{k+1}); \\ r_F = F(\boldsymbol{\sigma}^{k+1}, \Delta\lambda^{k+1}). \end{cases} \tag{12}$$

To solve the system of nonlinear Eqs. (12), Newton’s method (13) or linearization by Newton’s method (14) are used, the iterative procedures of which are respectively written as follows:

$$\begin{pmatrix} \boldsymbol{\sigma}_{j+1}^{k+1} \\ \Delta\lambda_{j+1}^{k+1} \end{pmatrix} = \begin{pmatrix} \boldsymbol{\sigma}_j^{k+1} \\ \Delta\lambda_j^{k+1} \end{pmatrix} - \left[ \begin{array}{cc} \frac{\partial \mathbf{r}_\sigma}{\partial \boldsymbol{\sigma}} & \frac{\partial \mathbf{r}_\sigma}{\partial \Delta\lambda} \\ \frac{\partial r_F}{\partial \boldsymbol{\sigma}} & \frac{\partial r_F}{\partial \Delta\lambda} \end{array} \right]^{-1} \begin{pmatrix} \mathbf{r}_\sigma^j \\ \mathbf{r}_F^j \end{pmatrix}, \tag{13}$$

or

$$\left[ \begin{array}{cc} \frac{\partial \mathbf{r}_\sigma}{\partial \boldsymbol{\sigma}} & \frac{\partial \mathbf{r}_\sigma}{\partial \Delta\lambda} \\ \frac{\partial r_F}{\partial \boldsymbol{\sigma}} & \frac{\partial r_F}{\partial \Delta\lambda} \end{array} \right] \begin{pmatrix} \delta\boldsymbol{\sigma}_j^{k+1} \\ \delta\Delta\lambda_j^{k+1} \end{pmatrix} = \begin{pmatrix} \mathbf{r}_\sigma^j \\ \mathbf{r}_F^j \end{pmatrix}, \begin{pmatrix} \boldsymbol{\sigma}_{j+1}^{k+1} \\ \Delta\lambda_{j+1}^{k+1} \end{pmatrix} = \begin{pmatrix} \boldsymbol{\sigma}_j^{k+1} \\ \Delta\lambda_j^{k+1} \end{pmatrix} + \begin{pmatrix} \delta\boldsymbol{\sigma}_j^{k+1} \\ \delta\Delta\lambda_j^{k+1} \end{pmatrix}. \tag{14}$$

Here, the index  $k$  refers to the loading step, and the index  $j$  refers to the number of iterations according to Newton’s method.

The use of linearization of a system of equations of the form (14) and its solution by the Gaussian elimination method instead of inverting the matrix in (13) using a unit matrix allows significantly reducing the number of arithmetic operations at each iteration step by approximately  $2n(n - 1)^2$ , where  $n$  is the dimension of the system of equations.

For  $k = 1$ , the usual elastic problem with respect to complete displacements under the boundary conditions (4)–(6) is solved and the tensor of test stresses is determined. Further, in the part of the body in the elastoplastic state, tensors of the increment of plastic deformations and elastic stresses are determined from solution (14) and the initial stresses are found by the formula

$$\boldsymbol{\sigma}^{0(k)} = \Delta\lambda^{(k)} \widehat{\mathbf{D}}^{el} \cdot \mathbf{m}^{(k)}. \quad (15)$$

The following integration steps (1), (2) for  $k > 1$  are performed only with a load with initial stresses (15), (16) under boundary conditions (4), i.e. without taking into account external and internal load. In this case, the elastic problem is also solved and the vector of increment of displacements  $\Delta\mathbf{u}^k$  is determined and the components of the vector of full displacements are determined, according to which new values of the components of the test stress tensor are found. Then, from solution (14), new values of the components of the tensors of the increment of plastic strains and elastic stresses are determined for the part of the body in the elastoplastic state. Next, to perform the next loading step, we find the tensor of the increment of initial stresses according to the formula

$$\boldsymbol{\sigma}^{0(k)} = \Delta\lambda^{(k)} \widehat{\mathbf{D}}^{el} \cdot \mathbf{m}^{(k)} - \boldsymbol{\sigma}^{0(k-1)}. \quad (16)$$

The plastic strain tensor is determined by the formula

$$\boldsymbol{\varepsilon}^{pl(k)} = \boldsymbol{\varepsilon}^{pl(k-1)} + \Delta\lambda^{(k)} \mathbf{m}^{(k)}.$$

The criterion for the completion of calculations may be the fulfillment of one of the conditions

$$|\Delta\mathbf{u}^k| \leq \delta_u \text{ or } \left| \boldsymbol{\varepsilon}_{eq}^{pl(k)} \right| \leq \delta_\varepsilon.$$

To apply the described methodology to the problems of the elastoplastic state of isotropic composite materials, it is necessary to determine their effective physical and mechanical properties. For this, one can either use the additive relations [13] using the known properties of the constituents (matrix and filler) of the composite or experimentally determine the effective values of these properties [7].

Additive relations [13] have the general form

$$P_{\text{comp}} = P_f V_f + P_m V_m,$$

where  $V_f$ ,  $V_m$  are the volume fractions of the filler and matrix, respectively; indices comp, f, m relate to the composite, filler, and matrix, respectively;  $P$  is one of the physical properties of the composite, filler, and matrix, respectively.

When solving the unbound thermo-elastic-plastic problem (7), which takes place in IG technology, to determine the temperature field, it is necessary either to solve the non-stationary (stationary) heat conduction problem with the corresponding initial and boundary conditions [14] or to set the known temperature field in advance.

### 3.3 Software Implementation of the Calculation Method

For the numerical implementation of the above algorithm, the finite element method (FEM) was used [9–12] and the Mathcad programming environment [15]. To build the

geometry and tetrahedron mesh of the model, free open source code is used – a CAD system for grid generation Gmsh [16]. To visualize the results of calculations of physical fields, the free open software code ParaView was used [17]. Testing of the developed program code for solving the problem of elastic-plasticity with isotropic hardening was performed using an example of a material with the mechanical properties of carbon steel.

To fulfill the conditions on the yield surface (11) with an accuracy of 10–6 in each plastic finite element (FE), iterations must be performed 6 times, and to achieve an accuracy of 0.1% in determining the components of the displacement vector, 10–15 loading steps are required initial stresses when solving the global system of discrete FEM equations.

**Test.** The problem of elasticity is taking into account the isotropic hardening of a thick-walled cylinder with radii  $r_1/r_2 = 0.05/0.08$  m. Material is steel ( $E = 2 \cdot 10^5$  MPa,  $\nu = 0.3$ ,  $\sigma_{y0} = 320$  MPa,  $h = 1.5 \cdot 10^3$  MPa). The pressure on the inner wall of the cylinder is  $p = 150$  MPa.

The grid convergence of the solution to the problem was determined by the double recount method. As a result, it was found that the computational grid of the test problem, consisting of 2041 linear tetrahedral FEs and 743 nodes, leads to an error in the determination  $\sigma_{eq}$  of not more than 0.5%.

**Table 1.** Results of a comparison of solutions to the plasticity problem taking into account isotropic hardening.

Type of solution	$u_s$ , m	$\sigma_{eq}$ , MPa	$\varepsilon_{eq}^{el}$	$\varepsilon_{eq}^{pl}$
ANSYS, nodes 774, FEs – 2209	$8.61 \cdot 10^{-5}$ – 0.000112	213–322	0.001064– 0.001608	0– 0.001217
Mathcad, nodes 743, FEs – 2041	$8.675 \cdot 10^{-5}$ – 0.00011204	215.3– 321.83	0.001076– 0.001607	0– 0.001218
Error, %	0.75–0.038	1.08– 0.053	1.13–0.06	0–0.08

Note:  $u_s = |\mathbf{u}|$  is the displacement vector module;  $\sigma_{eq}$  is Mises equivalent stresses;  $\varepsilon_{eq}^{el}$  and  $\varepsilon_{eq}^{pl}$  are equivalent Mises elastic and plastic deformations, respectively.

**Table 2.** The results of a comparison of the solutions of the plasticity problem for ideal plasticity.

Type of solution	$u_s$ , m	$\sigma_{eq}$ , MPa	$\varepsilon_{eq}^{el}$	$\varepsilon_{eq}^{pl}$
ANSYS, nodes 774, FEs – 2209	$8.62 \cdot 10^{-5}$ – 0.000113	213–320	0.001066– 0.0016	0–0.001128
Mathcad, nodes 743, FEs – 2041	$8.615 \cdot 10^{-5}$ – 0.0001111	212.8–320	0.001068– 0.00162	0– 0.00115825
Error, %	0.058–1.68	0.094–0	0.84–1.25	0–3.58

The results of a numerical solution of the elastoplastic problem for cases of isotropic hardening and ideal plasticity and their comparison with data obtained using the ANSYS Mechanical APDL software product [18] are given in Table 1 and 2.

The results of numerical modeling of physical fields in solving the test problem of elasticity using the developed software code confirm the possibility of its practical application.

### 4 Results

The following are the results of a numerical analysis of the elastic-plasticity of coke-pitch composite blanks in the production of isostatic graphite.

To conduct studies of thermo-elastic plasticity at the early stages of the burning of IG blanks, the composition of the coke-pitch composite was used, including calcined pitch coke as a filler with an average grain size of 15 μm and a matrix of high-temperature pitch (HTP) in an amount of 40% (by weight) [7]. The softening temperature of the HTP is 140 °C. Pitch coke is characterized by physical properties close to isotropic [19], which positively affects the properties of the finished IG. The calcination temperature of coke exceeds the burning temperature of the IG blanks, which minimizes its shrinkage during the heat treatment. The physical properties of the coke-pitch composite used in the calculations are given in Table 3.

**Table 3.** Physico-mechanical properties of IG blanks at the burning stage [7] (composition: calcined coke (15 μm) + 40% HTP).

$t, \text{ }^\circ\text{C}$	$\rho, \text{ kg/m}^3$	$c_p, \text{ J/(kg K)}$	$\lambda, \text{ W/(m}\cdot\text{K)}$	$E, \text{ MPa}$	$\sigma_c, \text{ MPa}$	$\sigma_t, \text{ MPa}$
20	1420	670	0.60	3800	12.0	3.1
100	1380	950	0.77	5000	12.0	3.1
200	1450	1180	0.90	8400	20.6	5.3

Note:  $t$  is temperature;  $\rho$  is density;  $c_p$  is mass isobaric heat capacity;  $\lambda$  is a coefficient of thermal conductivity;  $\sigma_c, \sigma_t$  are the compressive and tensile strengths, respectively.

In the calculations, the Poisson’s ratio, CLThE, the yield strength and the hardening modulus of the IG blanks were taken equal to  $\nu = 0.235, \beta = 1.8 \cdot 10^{-4} K^{-1}, \sigma_{y0} = 3 \text{ MPa}$  and  $h = 0 \text{ MPa}$ , respectively. When heated, the composite material of the IG blanks behaves differently: to the softening temperature of the pitch (matrices) expand, and after the onset of destruction, accompanied by gas-fission, it shrinks with the formation of semicoke and coke in the temperature range of more than 250 °C, which leads to an increase in its density [7, 20].



The calculations were performed for vertically standing IG blanks with a diameter of 300 mm and a height of 500 mm, taking into account gravitational and temperature loads on a finite element mesh consisting of 4762 linear tetrahedral FEs and 1311 nodes. The temperature load in the form of radial temperature drops across the workpieces varied within the range  $\Delta T_r = 5\text{--}15$  K.

Analysis of the calculation results shows that:

- a significant part of the IG blank under the influence of temperature loading is in the plastic state;
- in the upper part along the axis of the workpiece, gravitational compressive forces and temperature expansion cancel each other out, which results in minimal equivalent elastic deformations and, accordingly, equivalent Mises stresses.

Irreversible plastic deformations worsen the uniformity of the composite and provoke cracks nucleation at the initial stage of burning, i.e. to reach the level of softening temperatures of the matrix material, the beginning of destruction and intense gas evolution.

## 5 Conclusions

Tools have been developed in the form of methodology and software for the numerical study of the thermal-elastoplastic state of coke-pitch composites in the production technology of isostatic graphite.

Verification of the program code developed in the Mathcad environment is carried out using the example of a numerical solution of the test problem of the elastic-plasticity of isotropic material. A comparison of the results with the data of numerical analysis obtained using the ANSYS Mechanical APDL software product shows that, with isotropic hardening, the maximum discrepancy does not exceed 1.13%, and for ideal plasticity, it is no more than 3.58%.

A numerical analysis of the thermo-elastic-plastic state of composite IG blanks during the burning process is carried out. It is shown that in the early stages of burning at radial temperature gradients of large 33 K/m in the coke-pitch composite, undesirable plastic deformations may occur, which can contribute to the initiation of cracks and reduce the uniformity of the composite material.

## References

1. Chung, D.D.L.: Composite Materials: Science and Applications. Springer, London (2010). <https://doi.org/10.1007/978-1-84882-831-5>
2. Askeland, D.R., Phule, P.P.: The Science and Engineering of Materials, 5th edn. Thomson, Toronto (2006)
3. Kostikov, V., Samoylov, V., Beylina, N., Ostronov, B.: New high-strength carbon materials for traditional technologies. Russ. Chem. Mag. **48**(5), 64–75 (2004). (in Russian)

4. Asao, O.: High density isotropic graphites and glassy carbons. Japanese situation: production, properties and applications. Universidad de Alicante. Secretariado de Publicaciones, Alicante (1997)
5. Global Isostatic Graphite Market 2015 Industry Trends, Analysis & Forecast to 2020. QY Research, Florida (2015)
6. Karvatskii, A., Leleka, S., Pedchenko, A., Lasariev, T.: Investigation of the current state of isostatic graphite production technology. *Technol. Audit Prod. Reserves* **2/1**(34), 16–21 (2017)
7. Samoylov, V.: Receiving fine carbon fillers and development of the production technology of fine-grained graphites on their basis. Doctoral thesis, Research Institute of Constructional Materials on the Basis of Graphite «NIIGrafit», Moscow (2006). (in Russian)
8. Shuvalov, E.: About distribution of temperatures and thermal tension in carbon and graphite bodies of a cylindrical form. *Collect Works Chelyabinsk Electrometallurgical Plant* **2**, 200–214 (1970). (in Russian)
9. Simo, J., Taylor, R.: Consistent tangent operators for rate-independent elastoplasticity. *Comp. Methods Appl. Mech. Eng.* **48**, 101–118 (1985)
10. de Borst, R., Crisfield, M.A., Remmers, J.J., Verhoosel, C.V.: *Nonlinear Finite Element Analysis of Solids and Structures*. Wiley, New York (2012)
11. Zienkiewicz, O., Taylor, R., Fox, D.: *The Finite Element Method for Solid and Structural Mechanics*, 7th edn. Elsevier Ltd., Oxford (2014)
12. Karvatskii, A., Panov, E., Pedchenko, A., Shkil, V.: Modification of implicit algorithm for solving a problem on the elastic plasticity of bulk materials. *Eastern-European Journal of Enterprise Technologies* **5**(7(89)), 17–23 (2017)
13. Jones, R.: *Mechanics of Composite Materials*, 2nd edn. Taylor & Francis, Philadelphia (1999)
14. Karvatskii, A., Leleka, S., Pedchenko, A., Lazariev, T.: Numerical analysis of physical fields of graphitization process of electrode production in Castner's furnace. *East.-Eur. J. Enterp. Technol.* **6**(5(84)), 19–25 (2016)
15. PTC Mathcad. <https://www.ptc.com/en/products/mathcad>. <http://www.ptc.com/engineering-math-software/mathcad/>. Accessed 29 May 2019
16. Gmsh: a three-dimensional finite element mesh generator with built-in pre- and post-processing facilities. <http://gmsh.info/>. Accessed 29 May 2019
17. ParaView. <https://www.paraview.org/>. Accessed 29 May 2019
18. Thompson, M., Thompson, J.: *ANSYS Mechanical APDL for Finite Element Analysis*. Butterworth-Heinemann, Oxford (2017)
19. Ostrovskiy, V., Beylina, N., Lipkina, N., Sinelnikov, L.: Peak coke as filler of constructional graphites. *Chem. Solid Fuel* **1**, 56–61 (1995)
20. Gromov, B., Panov, Ye., Bozhenko, M., Vasilchenko, G., Karvatskii, A., Shilovich, I.: *Burning and Start of Aluminum Electrolyzers*. Ore and Metals Publishing House, Moscow (2001)